Progress In Electromagnetics Research M, Vol. 61, 97–110, 2017

An Efficient Technique for Digital Video Broadcasting Using High-Altitude Aerial Platforms and Adaptive Arrays

Yasser Albagory[1, 2, *]

Abstract—In this paper, an efficient broadcasting technique for digital-video and audio broadcasting (DVB/DAB) is proposed using High-Altitude Platforms (HAP) and a new adaptive beamforming technique. The proposed beamforming technique uses two cascaded weighting functions to generate uniform flat footprint with improved link performance compared to terrestrial systems. These two weighting functions include flattening and smoothing coefficients to generate flat power distribution with lower sidelobe levels. Simulation results show that the generated coverage beam pattern has low sidelobe levels that is more than 40 dB below the main coverage level with less than 1 dB variation over the main coverage lobe level. Also, an almost uniform bit-energy to noise power spectral density can be achieved over the coverage area with minor variations due to the changing slant distance over the coverage area of broadcasting HAP.

1. INTRODUCTION

Digital broadcasting such as Digital Video Broadcasting (DVB) and Digital Audio Broadcasting (DAB) are very important applications where they provide users with various information and services [1]. These services include daily information news, entertainment, sports, and many other programs. Both terrestrial and satellite communications systems are used to broadcast DVB and DAB, and each has its own advantages and disadvantages [2, 3]. For example, terrestrial broadcasting systems require simple receivers without complicated antenna installations but suffers from severe propagation losses which depend on the terrains of the coverage area and weather conditions that result in small coverage areas. Therefore, terrestrial digital broadcasting services are limited in performance by the terrestrial propagation channel impairments such as multipath fading, rain, and fog. On the other hand, broadcasting satellite systems provide wider coverage areas where a single geostationary satellite at 36000 km altitude from Earth can provide 42% of the earth's surface. In addition, satellite communication channel is characterized by free-space propagation models which have better link and attenuation performance. The main disadvantage of satellite communication systems is the huge free space loss due to the large slant distance between receivers and satellite especially for geostationary orbit satellites which require special receiving and transmitting dish antenna installations. Recently, High-Altitude Platforms (HAP) is proposed for many communications applications including the provision of mobile, data, and surveillance services [4, 5]. HAP is an airship that can be positioned at altitudes in the stratosphere especially 20 km high and can provide many communications services as interrestrial and satellite systems. Mobile communications can be provided using the same cellular topologies as in the terrestrial systems but with much better performance [6]. HAP communications provide many advantages compared with conventional satellite and terrestrial systems such as wide coverage with lower propagation loss than terrestrial systems and easier upgrading and maintenance operations than

Received 24 August 2017, Accepted 11 October 2017, Scheduled 23 October 2017
* Corresponding author: Yasser Albagory (dalbagory@gmail.com).
[1] College of Computers and Information Technology, Taif University, Saudi Arabia. [2] Faculty of Electronic Engineering, Menoufia University, Egypt.

satellites. In this paper, HAP technology is combined with a new adaptive antenna beamforming technique to improve the performance of digital broadcasting services. The proposed system is composed of stratospheric HAP station that is equipped with an adaptive antenna array system designed for flat power pattern with lower sidelobe levels. The paper is arranged as follows. Section 2 describes the architecture of the HAP broadcasting system. Section 3 proposes and discusses the adaptive antenna beamforming technique for HAP digital broadcasting. Section 4 analyzes the HAP footprint and performance of the communications link while Section 5 discusses the simulation results. Finally, Section 6 concludes the paper.

2. HAP DIGITAL BROADCASTING SYSTEM

In the HAP communications system, the advantage of being nearer to Earth than satellite provides very low free-space attenuation where the minimum slant distance of the Geostationary satellite is 36000 km while it is only 20 km in the case of HAP located in the stratosphere. As shown in Fig. 1, a single HAP can be used in broadcasting services where it can cover an area of several hundreds of kilometers diameter. A single HAP located at 20 km high can cover a circular area of up to 1000 km diameter which is very huge compared to conventional terrestrial broadcasting towers. The system architecture as shown in Fig. 1 is very similar to the conventional satellite broadcasting system where the HAP is considered as a satellite positioned at 20 km high in the stratosphere. A ground station transmits the broadcast channels that are relayed to a wider area on the ground by the HAP. This ground station also performs the telemetry, tracking and telecommand (TTC) operations for positional stability and control of the HAP as in satellite control ground stations. In satellite systems, the huge distance between satellite and Earth limits the antenna array beamforming capabilities where conventional horn or reflector type antennas are usually used. On the other hand, in the HAP broadcasting system, efficient beamforming techniques can be proposed and applied to gain more improvement in system performance as will be discussed in the subsequent sections.

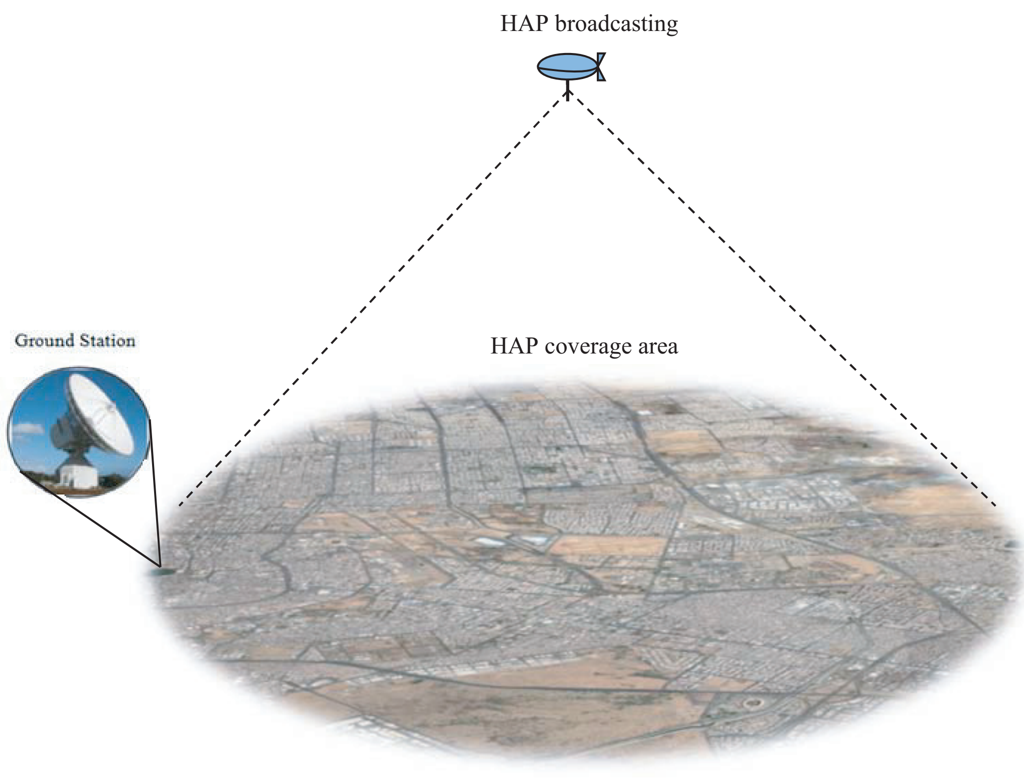

Figure 1. HAP digital broadcasting system.

3. ANTENNA ARRAY STRUCTURE AND BEAMFORMING TECHNIQUE FOR HAP-BASED DIGITAL BROADCASTING SYSTEM

Conventional satellite broadcasting system utilizes spot-beam directional antennas such as horn and parabolic reflector antennas to provide the required gain and footprint over the coverage area [7, 8]. Also, antenna arrays [9] can be applied to shape the coverage beams over the required area where an array of horn antennas are spotted over the required area to shape the radiation pattern. Another sophisticated method is to shape the surface of the reflector to control the footprint contours [10]. In this section, the height of HAP stations is much lower relative to satellites which provides more flexibility in using variety of antenna beamforming techniques and types. Linear antenna arrays are applied in this paper, and the HAP station in this case is similar to a very high tower that can provide wide area coverage as in satellite systems.

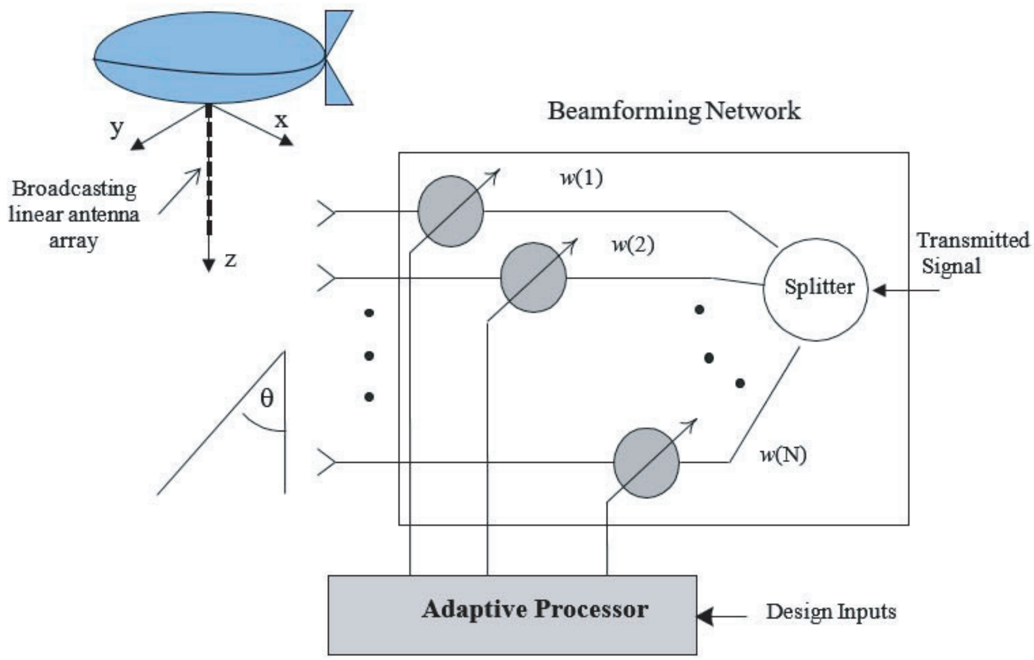

Figure 2. Beamforming system for the vertical broadcasting array onboard AP.

The array structure onboard the HAP station is shown in Fig. 2 where the elements are arranged vertically on the z-axis. The elements spacing is set to a half-wavelength distance. The antenna elements are fed through a beamforming network where the HAP transmitted signals are controlled in magnitude and phase to achieve the required power pattern. The flat or uniform power gain over the coverage area is very important for simplifying the receivers design requirements and for making indoor reception possible even at the coverage area boundaries. Conventional terrestrial broadcasting systems have signal power levels that fall rapidly with distance which requires compensation by the receivers. Therefore, if the power distribution over the covered area is almost uniform, then the receiver compensation for power degradation at different locations is minimal; the quality of reception can be improved; the system will be more immune to propagation impairments such as rain or fog absorption than terrestrial and satellite systems.

The design of uniform power pattern over the coverage area can be achieved by proposing a form of weighting function, $\omega(n)$, that consists of two parts as follows:

$$\omega\left(n\right) = \omega_f(n)\omega_s(n) \tag{1}$$

where $\omega_f(n)$ is a flattening function responsible for the uniform power coverage, $\omega_s(n)$ a smoothing function that reduces the ripples in the power pattern over the coverage area, and n the element number.

The flattening function $\omega_f(n)$ is proposed in a form of $\sin(x)/x$ function as follows:

$$\omega_f\left(n\right)=\frac{\sin\left(\mu\theta_c\left(n-\dfrac{N+1}{2}\right)\right)}{\mu\theta_c\left(n-\dfrac{N+1}{2}\right)} \tag{2}$$

where μ is a coverage adjustment factor that controls actual coverage diameter and ranges from 0.5 to 1, and θ_c is the coverage beamwidth in radians, calculated from the following equation:

$$\theta_c=2\tan^{-1}\left(\frac{D_c}{2h}\right) \tag{3}$$

where D_c is the coverage area diameter and h the HAP height.

The function $\omega_s(n)$ is proposed to be a tapering window as follows:

$$\omega_s\left(n\right)=e^{\frac{-\left(n-\frac{N+1}{2}\right)^2}{N^{\delta}}} \tag{4}$$

where δ is a smoothing factor ranging from 1 to 2 which controls the tapering profile of $\omega_s(n)$, and N is the total number of array antenna elements.

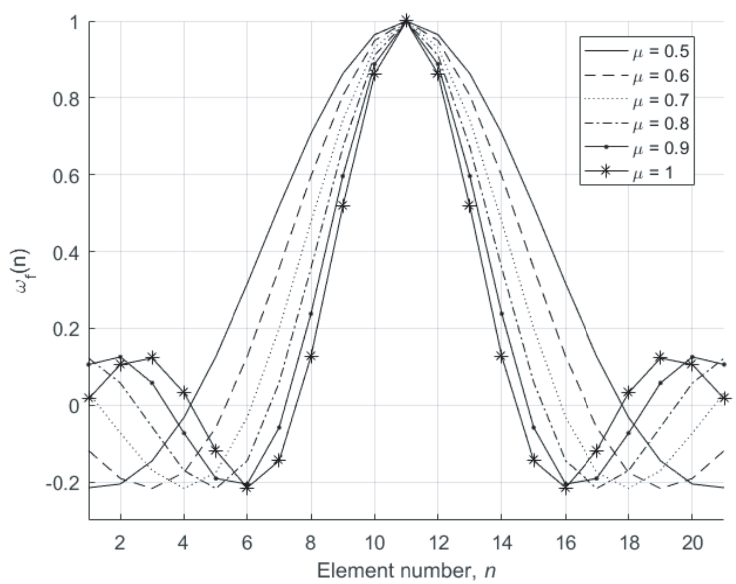

Figure 3. Flattening function profile at different beamwidth control factor (μ).

The two weighting functions are drawn in Figs. 3 and 4 as a function of the element number, n, and at different values of μ and δ respectively for a 21-element linear vertical array. In Fig. 3, decreasing the value of μ decreases the rate of variation of $\omega_f(n)$ at a specific coverage beamwidth θ_c while in Fig. 4, the curve is broadened more by increasing the value of δ. At $\delta > 2$, the smoothing function will be almost flat and has no effect on the overall weighting function $\omega(n)$. The overall weighting function for an array of 21 elements at $\mu = 0.9$ and $\delta = 1.5$ is drawn in Fig. 5 where the flattening weights and the final weights are compared. This figure shows minimal difference between the two functions which has an important effect on reducing the ripples in the array power gain as will be discussed in the next section.

4. ARRAY POWER GAIN AND E_b/N_o FOOTPRINTS

Consider an HAP that is located at h km altitude as shown in Fig. 1 and equipped with a linear antenna array system as shown in Fig. 2. The array power pattern is designed to have a 3 dB beamwidth of θ_c

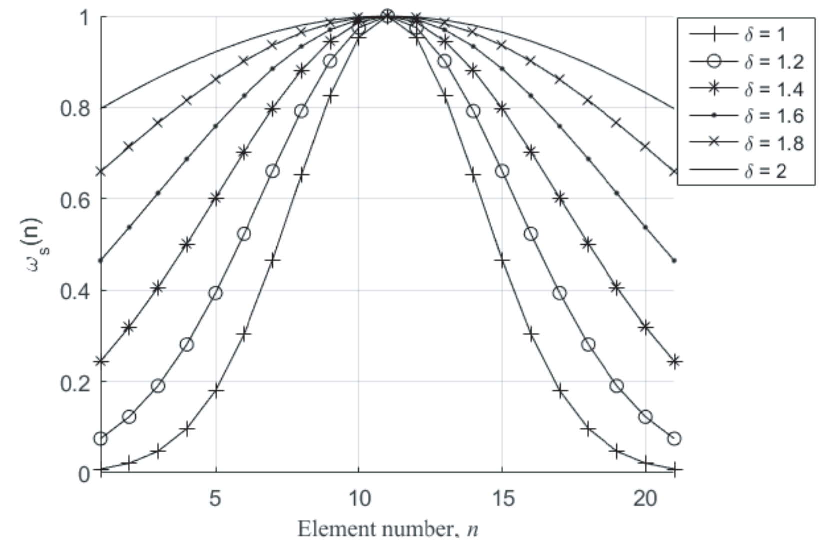

Figure 4. Smoothing function profile at different smoothing factor (δ).

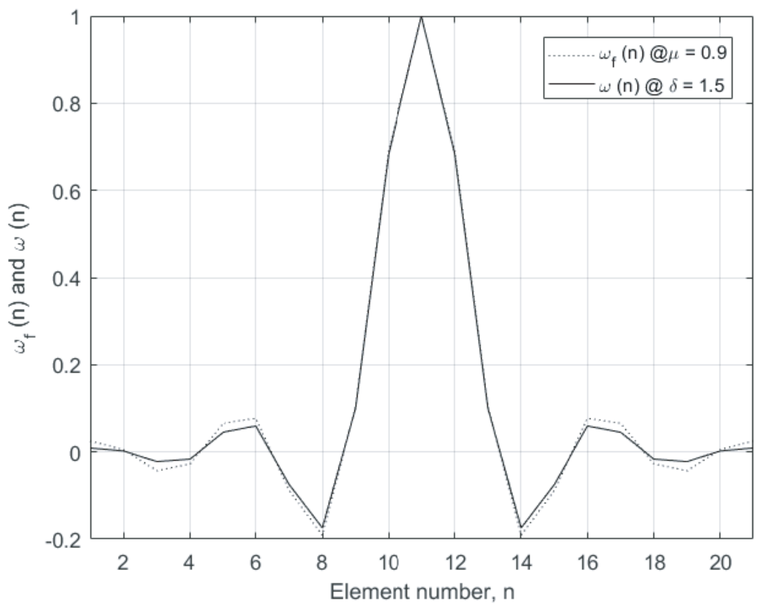

Figure 5. Overall weighting and flattening function profiles.

which is obtained by performing fine adjustment of the weights in Eq. (1). The array will be oriented downward along an inverted z-axis, and the corresponding array steering vector, $S_L(\theta)$, can be written as:

$$S_L\left(\theta\right) = \begin{bmatrix} 1 \\ e^{j\pi\cos(\theta)} \\ e^{j2\pi\cos(\theta)} \\ \vdots \\ e^{j(N-1)\pi\cos(\theta)} \end{bmatrix} \tag{5}$$

The array steering vector in Eq. (5) has a unity column vector at $\theta = 0^\circ$, which means that the maximum array gain will be at the coverage center. The weights are then combined with the unity steering vector $S_L(0)$ and multiplied by the steering vector at any direction θ to determine the array factor $AF(\theta)$ as follows:

$$AF\left(\theta\right)=\sum_{n=1}^{N}\omega^{*}\left(n\right)e^{j\pi(n-1)\cos(\theta)} \tag{6}$$

And the array power gain will be:

$$G_{t}\left(\theta\right)=\left|\sum_{n=1}^{N}\omega^{*}\left(n\right)e^{j\pi(n-1)\cos(\theta)}\right|^{2} \tag{7}$$

where $\omega^{*}(n)$ is the complex conjugate of the weighting function $\omega(n)$.

The received power level can be written as:

$$P_{r}\left(\theta\right)=P_{t}G_{t}\left(\theta\right)G_{r}\left(\theta\right)\left(\frac{\lambda}{4\pi d\left(\theta\right)}\right)^{2}\frac{1}{X_{L}} \tag{8}$$

where P_t is the input transmitted power at HAP, $G_r(\theta)$ the receiving antenna power gain, $(\frac{\lambda}{4\pi d(\theta)})^2$ the free space path loss, λ the wavelength in meter, $d(\theta)$ the slant distance from the HAP location to the receiver location, and X_L an extra loss due to other factors including fading margin and absorption losses.

A favorable representation for $P_r(\theta)$ is using decibel form as follows:

$$P_{r}\left(\theta\right)\text{ dB}=P_{t}\,\text{dB}+G_{t}\left(\theta\right)\text{ dB}+G_{r}\left(\theta\right)\text{ dB}-20\log\left(\frac{4\pi d\left(\theta\right)}{\lambda}\right)-X_{L}\,\text{dB} \tag{9}$$

On the other hand, the required input power at the transmitting HAP antenna system can be written as:

$$P_{t}\,\text{dB}=P_{r}\left(\theta\right)\text{ dB}-G_{t}\left(\theta\right)\text{ dB}-G_{r}\left(\theta\right)\text{ dB}+20\log\left(\frac{4\pi d\left(\theta\right)}{\lambda}\right)+X_{L}\,\text{dB} \tag{10}$$

If we assume simple omnidirectional receiving antenna ($G_r(\theta)\,\text{dB} = 0\,\text{dB}$), then the received power is affected by the HAP antenna power pattern $G_t(\theta)\,\text{dB}$ and slant distance $d(\theta)$ assuming that other factors are constant.

The slant distance $d(\theta)$ can be calculated from Fig. 6 as follows:

$$d\left(\theta\right)=\left(h+R_{e}\right)\cos\left(\theta\right)-\sqrt{R_{e}^{2}-\left(h+R_{e}\right)^{2}\left(\sin\left(\theta\right)\right)^{2}} \tag{11}$$

where R_e is the Earth's radius, E the receiver location, and O the Earth's center.

One of the key performance measurement factors for digital communication systems is the ratio of bit-energy-to-noise power spectral density ($\frac{E_b}{N_o}$) which determines the probability of error according to the applied digital modulation technique. The ratio of $\frac{E_b}{N_o}(\theta)$ will be a function of the received signal power which depends on the receiver location, bit rate (R_b) and noise power spectral density (N_o) as follows:

$$\frac{E_{b}}{N_{o}}\left(\theta\right)=\frac{P_{r}(\theta)}{R_{b}N_{o}} \tag{12}$$

where $N_o = KT$, K is the Boltzmann's constant and T the noise temperature in Kelvins.

$\frac{E_b}{N_o}(\theta)$ is usually expressed in dB as follows:

$$\frac{E_{b}}{N_{o}}\left(\theta\right)\text{ dB}=P_{r}\left(\theta\right)\text{ dB}-10\log\left(R_{b}\right)-10\log(N_{o}) \tag{13}$$

Or

$$\frac{E_{b}}{N_{o}}\left(\theta\right)\text{ dB}=P_{t}\,\text{dB}+G_{t}\left(\theta\right)\text{ dB}+G_{r}\left(\theta\right)\text{ dB}-20\log\left(\frac{4\pi d\left(\theta\right)}{\lambda}\right)-X_{L}\,\text{dB}-R_{b}\,\text{dB}-N_{o}\,\text{dB} \tag{14}$$

Eq. (14) indicates that the system performance can be improved by improving $\frac{E_b}{N_o}(\theta)\,\text{dB}$, and to achieve this goal, we should improve the transmitting antenna gain ($G_t(\theta)\,\text{dB}$) and its profile over the coverage area. The other factors $P_t\,\text{dB}$, $G_r(\theta)\,\text{dB}$, $20\log(\frac{4\pi d(\theta)}{\lambda})$, $X_L\,\text{dB}$, $R_b\,\text{dB}$, and $N_o\,\text{dB}$ are considered constant or fixed for comparison purposes.

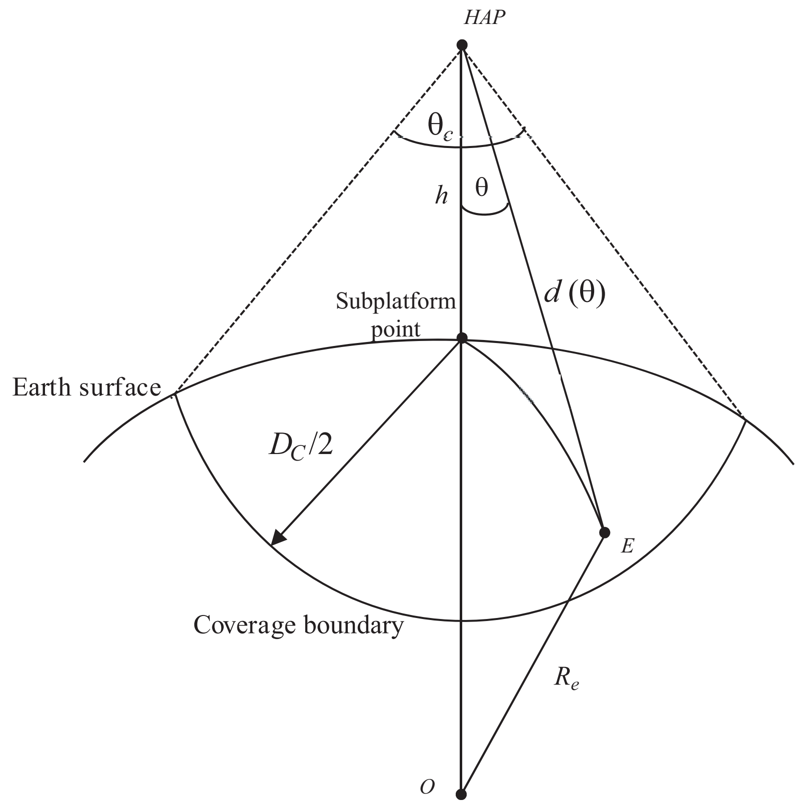

Figure 6. Geometry of HAP broadcasting system for slant range calculation.

5. RESULTS AND DISCUSSIONS

In this section, we describe the design of an HAP broadcasting system using the proposed antenna beamforming technique. The design factors and their effects on the antenna power pattern as well as the footprint of $\frac{E_b}{N_o}(\theta)$ dB will be also discussed. The results are obtained by using MATLAB software with a platform of i7-6700 HQ processor @2.6 GHz and 16 GB RAM. According to the 1 km resolution, the power pattern is calculated over a square area of 200 km side length, and the approximate calculation time is about 10 seconds and is affected by the array size and power pattern resolution as well as the coverage area diameter.

5.1. Normalized Array Power Gain

As a case study, we consider a design of HAP broadcasting system to cover an area of 100 km diameter using a linear antenna array of the following design parameters: $N = 51$, $\mu = 0.86$, and $\delta = 1.6$. The normalized power pattern is obtained by using the normalized weights in Fig. 7 obtained from the following equation:

$$\omega_N(n) = \frac{\omega(n)}{\sum_{i=1}^{N} \omega(i)} \tag{15}$$

Figure 8 displays the normalized array power pattern which is uniform over the coverage area with omnidirectional pattern (i.e., independent on azimuth direction). The sidelobe performance can be depicted clearly in Fig. 9 where it falls to less than -40 dB below the main coverage level. The sidelobe floor of -40 dB provides excellent isolation between coverage areas that use the same set of broadcasting channels frequencies.

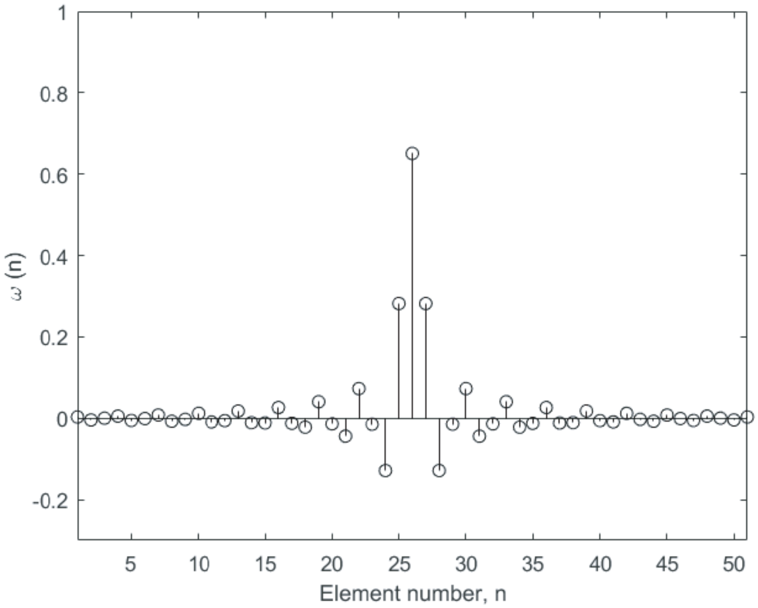

Figure 7. Weighting function profile for 100 km diameter coverage for HAP at 20 km high.

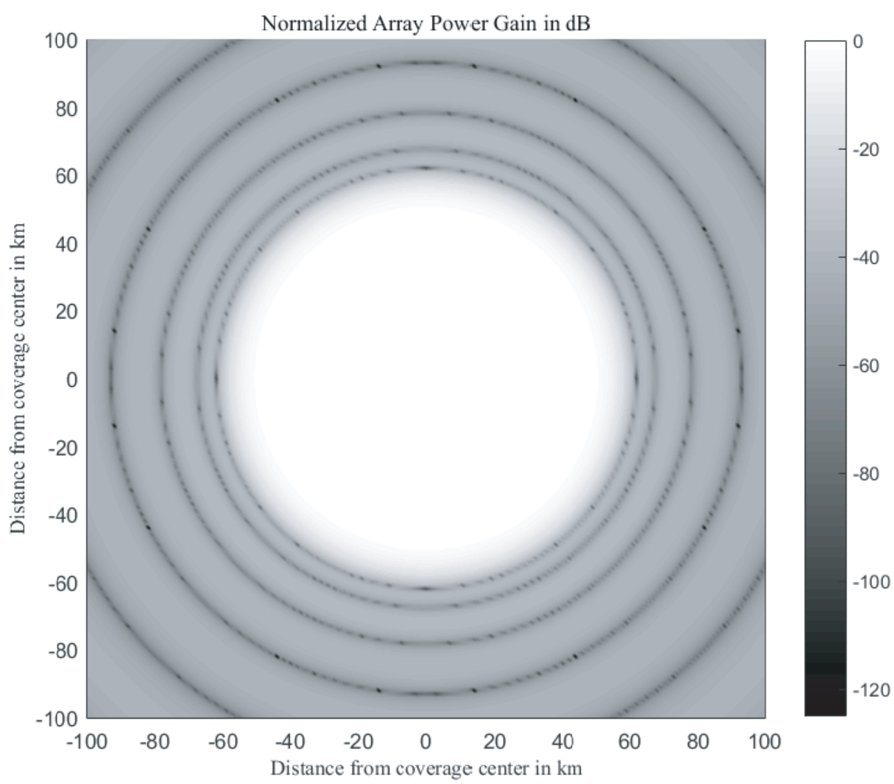

Figure 8. Normalized array power gain in dB.

5.2. HAP E_b/N_o Footprint

The impact of the transmitting antenna gain on $\frac{E_b}{N_o}$ is depicted by plotting $\frac{E_b}{N_o}(\theta)$ dB as shown in Figs. 10 and 11 where the DVB-T parameters are applied including 700 MHz carrier frequency, 5 MHz channel bandwidth and QPSK modulation. Fig. 10 displays the almost uniform footprint of $\frac{E_b}{N_o}(\theta)$ dB, and

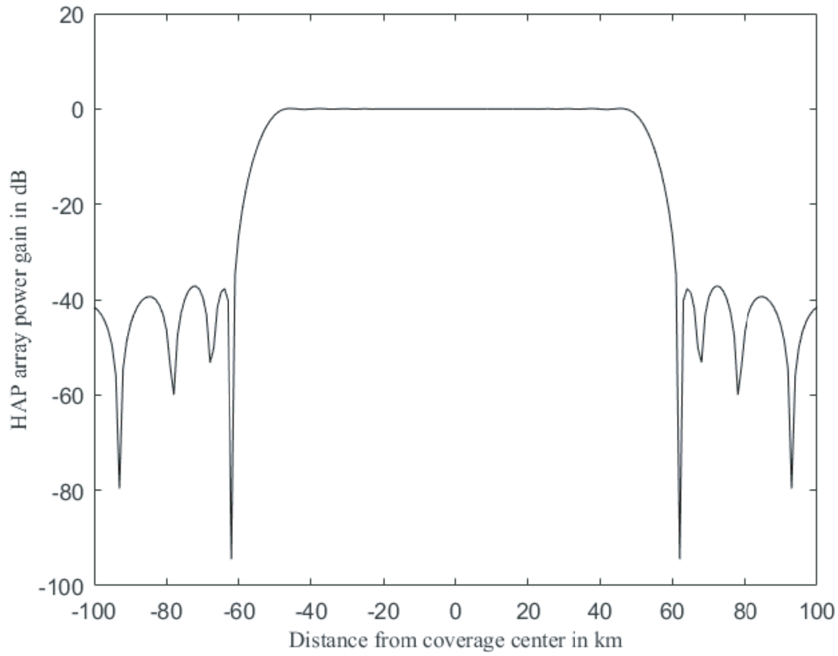

Figure 9. Profile of the normalized array power gain in dB.

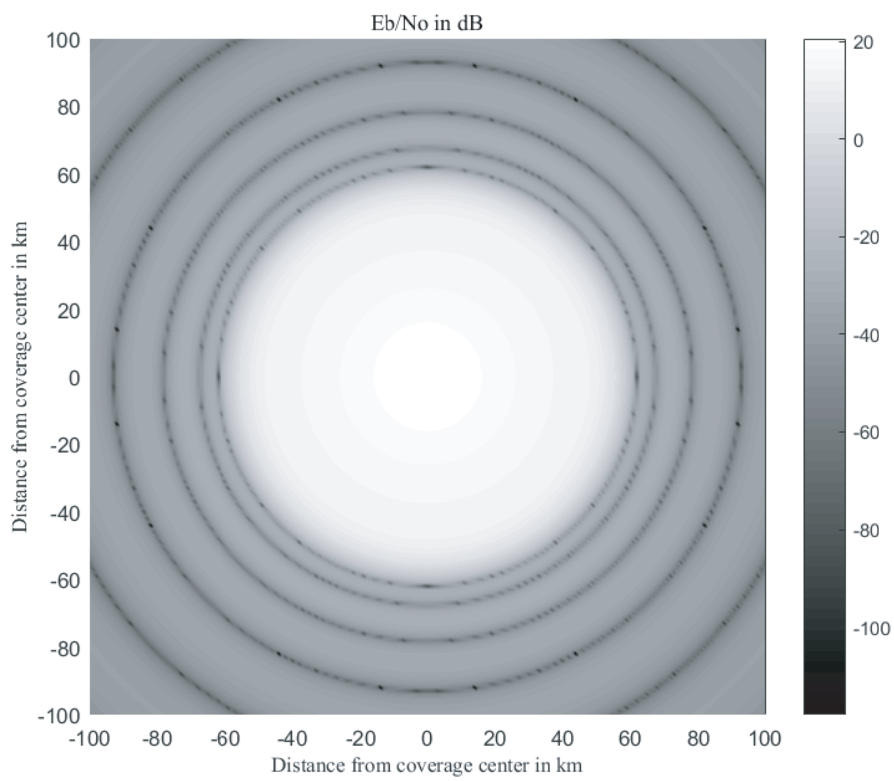

Figure 10. Footprint of HAP $\frac{E_b}{N_o}$ in dB.

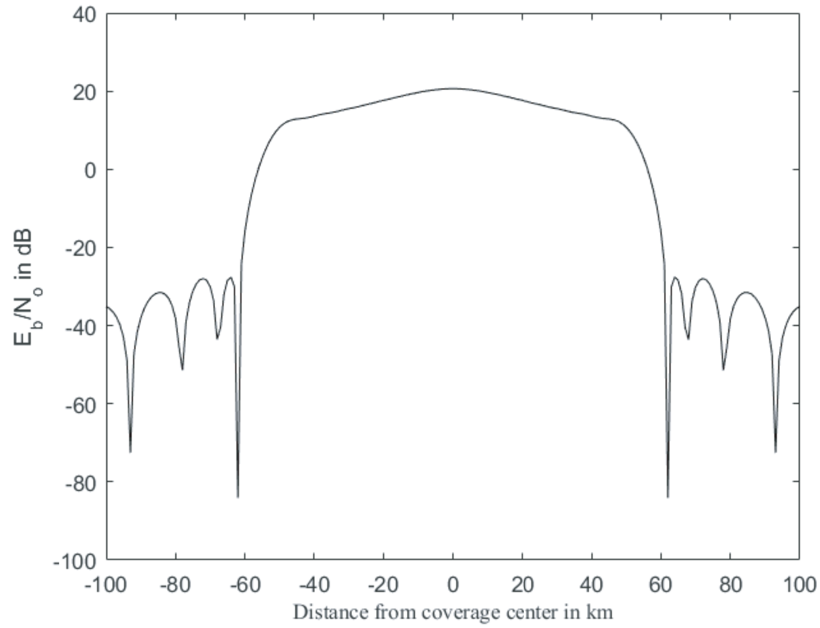

Figure 11. Profile view of the HAP $\frac{E_b}{N_o}$ in dB.

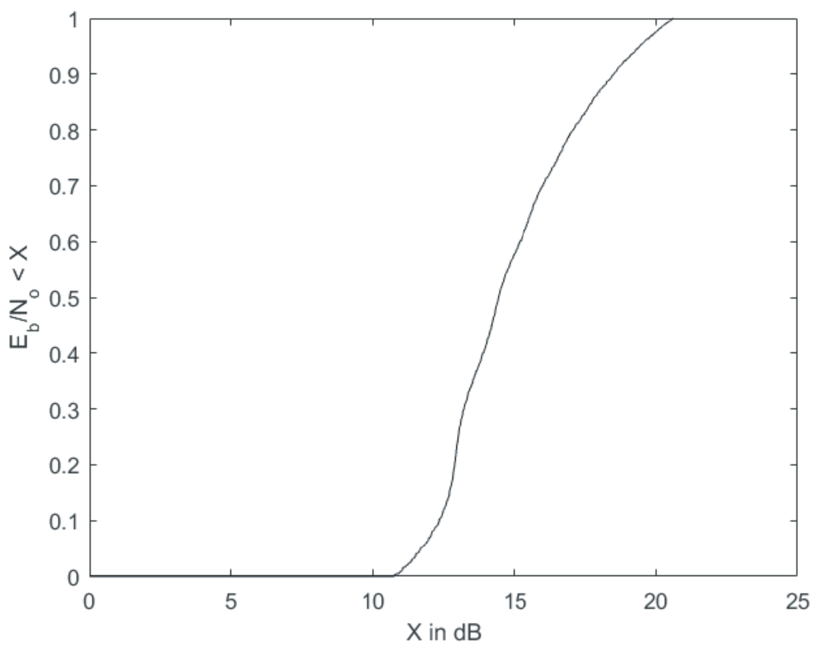

Figure 12. The part of $\frac{E_b}{N_o}$ that is lower than X with X.

Fig. 11 shows a very small slope due to the slant distance variation over the coverage area where it ranges from 20 at the subplatform point to 54 km at the boundary of the coverage area.

The almost uniform or flat HAP $\frac{E_b}{N_o}$ footprint guarantees the good quality of reception throughout the coverage area.

The percentage or probability of the area that $\frac{E_b}{N_o}$ is greater than specific value is another performance representation of the quality of coverage as shown in Fig. 12 where the steep curve means almost uniform distribution of $\frac{E_b}{N_o}$, and a minimum guaranteed value of 11 dB is achieved.

5.3. Comparison with Omnidirectional Antenna and Simple Two-Element Array

The uniform power pattern can be obtained by other variant antenna structures such as the isotropic or omnidirectional antenna where the constant radiation pattern is achieved. In Fig. 13, three antenna power patterns are compared including the proposed beamforming technique, omnidirectional antenna, and two-element uniform array spaced by half-wavelength. The omnidirectional antenna is chosen as a reference for the uniform coverage, and the two-element antenna array is also chosen as the array that gives the widest beamwidth that is very close to the omnidirectional antenna performance with the

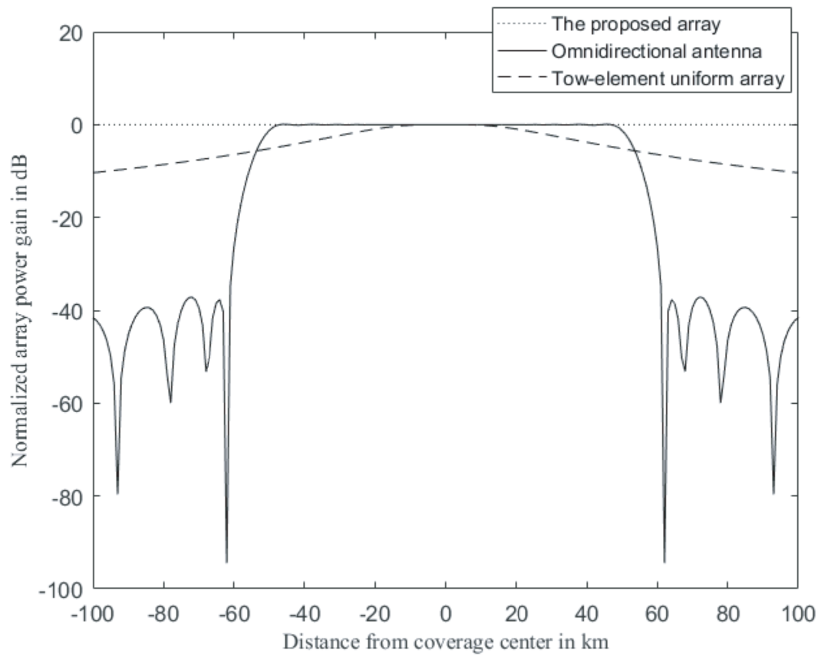

Figure 13. Normalized antenna power gain of three antenna systems for aerial coverage from HAP.

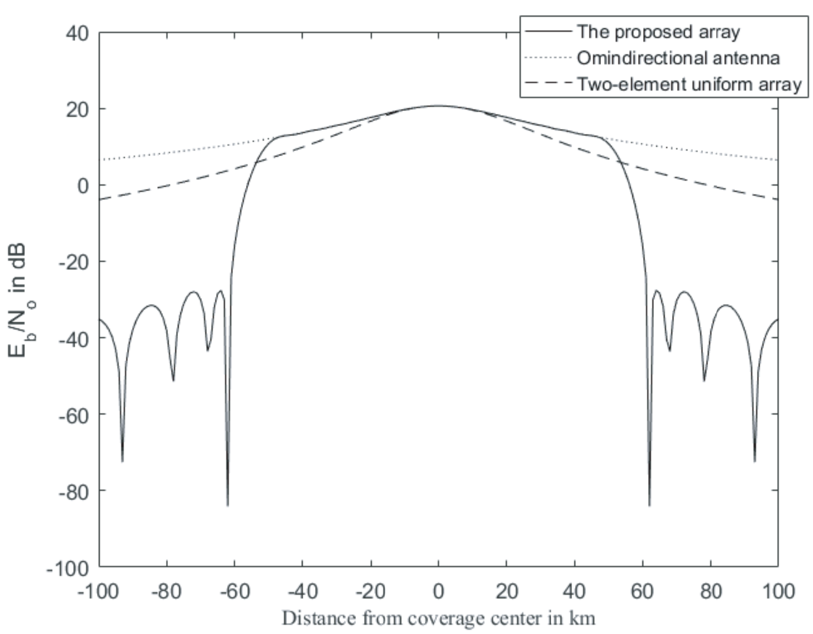

Figure 14. $\frac{E_b}{N_o}$ profile for three antenna systems for aerial coverage from HAP.

minimum number of antenna elements. The proposed technique has the capability of controlling the size of the coverage area with very low sidelobe levels. The impact of the three techniques on $\frac{E_b}{N_o}$ is shown in Fig. 14 where the proposed technique has identical performance to the omnidirectional antenna over the coverage area which confirms the uniformity of the coverage. The performance degrades for the uniform two-element array due to its smaller beamwidth.

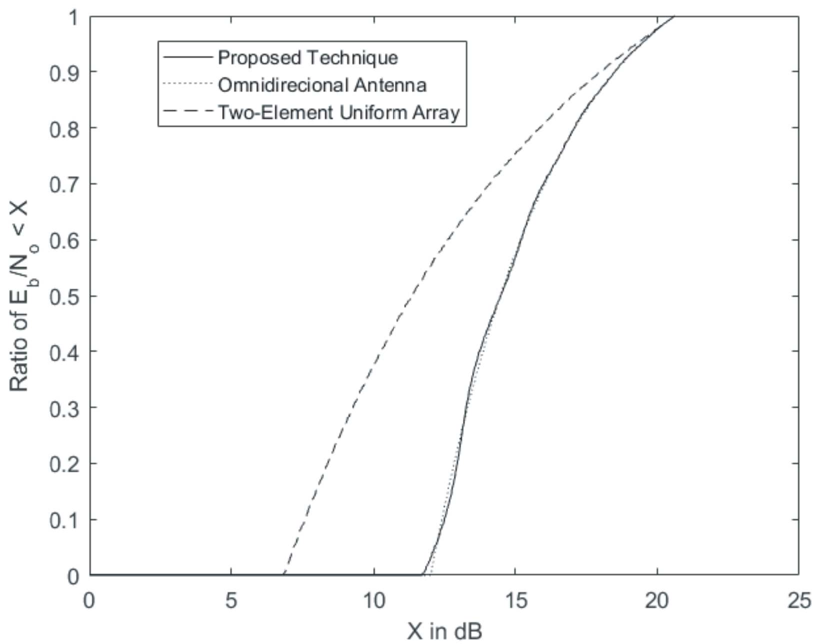

Figure 15. The part of $\frac{E_b}{N_o}$ that is lower than X with X of three antenna systems for aerial coverage from HAP.

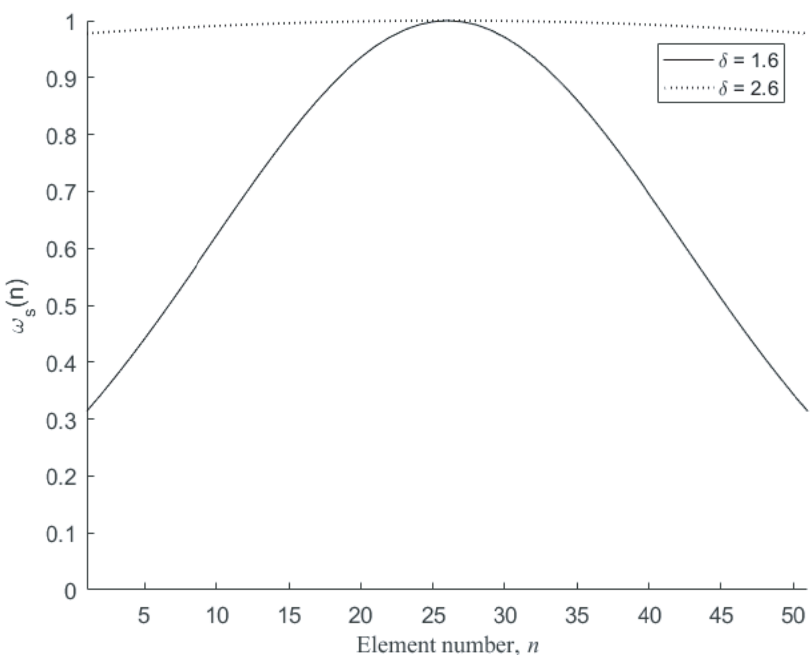

Figure 16. Smoothing function profile at two different values of δ.

The distribution of $\frac{E_b}{N_o}$ over the coverage area of Fig. 14 is confirmed in Fig. 15 where the steeper performance of the proposed array is almost identical to the omnidirectional antenna over the coverage area and degrades for the two-element uniform array. The minor variations between the proposed array technique and the omnidirectional antenna in the coverage area is due to the minor ripples in the power pattern of the proposed antenna technique.

5.4. Effects of δ on the Array Power Pattern

The impact of δ on the array performance is very important and should be investigated where it controls both the sidelobe level and ripple width in the array gain over the coverage area (i.e., main lobe). As mentioned before, the value of δ ranges from 1 to 2, and its effect on the power pattern is negligible at values greater than 2.6. To describe the effect of δ on the array power pattern, we use two values of δ (1.6 and 2.6) as shown in Fig. 16 to achieve 100 km coverage diameter. At $\delta = 2.6$ the smoothing effect is negligible, and the weights are almost the same as the flattening weights while the tapered profile of $\omega_s(n)$ at $\delta = 1.6$ greatly affects the performance of the array especially the sidelobe levels and reduces the ripples in the normalized array power pattern over the coverage area. As shown in Fig. 17, the sidelobe levels are lower by about 19 dB when $\delta = 1.6$ than at $\delta = 2.6$.

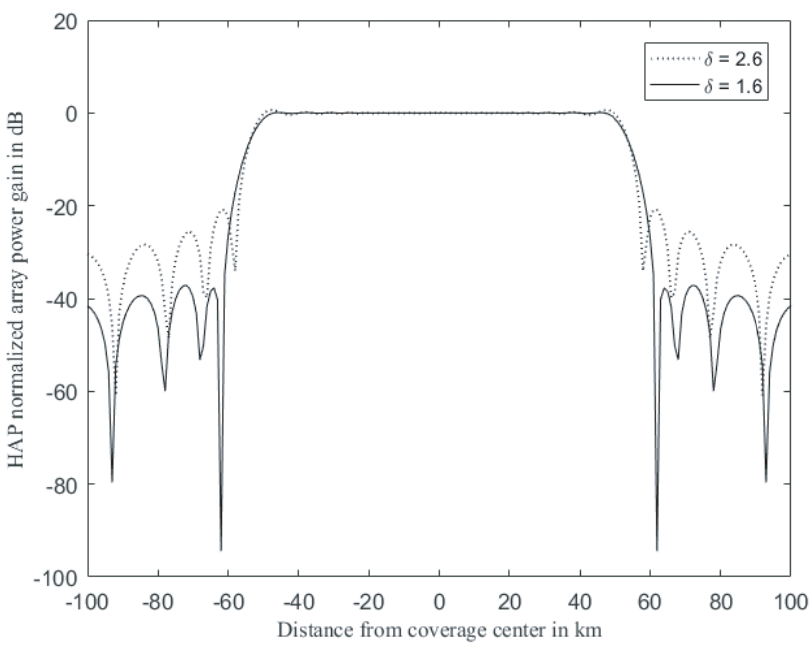

Figure 17. Effect of the smoothing function on the normalized array power gain.

6. CONCLUSION

In this paper, an efficient digital broadcasting using adaptive beamforming and HAP has been proposed where uniform flat coverage with improved link performance has been achieved. The synthesized array pattern has uniform flat coverage with very low sidelobe levels that is necessary for reducing the interference at the other neighboring co-channel regions. Sidelobe levels that are below the main lobe gain by 40 dB have been achieved theoretically using a 51-element array with less than 1 dB ripples in the mainlobe gain over 100 km coverage diameter. The proposed beamforming technique has improved the link performance in terms of bit-energy-to-noise power spectral density levels with almost uniform distribution over the coverage area with minor degradation due to the slant distance variation.

REFERENCES

1. Fischer, W., *Digital Video and Audio Broadcasting Technology, a Practical Engineering Guide*, 3rd edition, Springer, 2011.
2. Zhang, M. and S. Kim, "Efficient soft demodulation scheme for digital video broadcasting via satellite second generation system," *IET Communications*, Vol. 8, No. 1, 124–132, Jan. 3, 2014.
3. Oria, C., V. Baena, J. Granado, J. García, D. Pérez-Calderón, P. López, and D. Ortiz, "Performance evaluation of complementary code combining diversity in DVB-SH," *Digital Signal Processing*, Vol. 21, No. 6, 718–724, Dec. 2011.
4. Karapantazis, S. and F. Pavlidou, "Broadband communications via high-altitude platforms: A survey," *IEEE Communications Surveys & Tutorials*, Vol. 7, 2–31, 2005.
5. Mohammed, A. and Z. Yang, "Broadband communications and applications from high altitude platforms," *International Journal of Recent Trends in Engineering*, Vol. 1, No. 3, May 2009.
6. Aljahdali, S., M. Nofal, and Y. Albagory, "Overview on modeling and design of stratospheric mobile cellular system," *IEEE International Conference on Multimedia Computing and Systems (ICMCS'12)*, Tangier, Morocco, 2012.
7. Fauzi, N. F., M. T. Ali, N. H. A. Rahman, and Y. Yamada, "Optimized parabolic reflector antenna for Malaysia beam coverage," *2016 IEEE Asia-Pacific Conference on Applied Electromagnetics (APACE)*, 150–153, Langkawi, 2016, doi: 10.1109/APACE.2016.7915873.
8. Hosseini, A., S. Kabiri, and F. De Flaviis, "V-band high-gain printed quasi-parabolic reflector antenna with beam-steering," *IEEE Transactions on Antennas and Propagation*, Vol. 65, No. 4, 1589–1598, Apr. 2017, doi: 10.1109/TAP.2017.2670324.
9. Rocca, P. and A. F. Morabito, "Optimal synthesis of reconfigurable planar arrays with simplified architectures for monopulse radar applications," *IEEE Transactions on Antennas and Propagation*, Vol. 63, No. 3, 1048–1058, 2015.
10. Wu, J.-M., X. Lei, D.-F. Zhou, L. Hou, and H.-W. Chen, "Design of ring-focus elliptical beam reflector antenna," *International Journal of Antennas and Propagation*, Vol. 2016, 7 pages, Article ID 9615064, 2016, doi:10.1155/2016/9615064.